Aluminophosphates

In Situ UV Raman Spectroscopic Study on the Synthesis Mechanism of AlPO-5**

Fengtao Fan, Zhaochi Feng, Keju Sun, Meiling Guo, Qiang Guo, Yu Song, Weixue Li, and Can Li*

Research on crystalline models of aluminophosphate molecular sieves as well as many other metallophosphates was initiated by the pioneering works on the synthesis of 1D chain and ladder structures[1] that subsequently develop into 2D and finally complex, 3D architectures.[2–4] The work of Oliver et al. undoubtedly promoted the understanding of the synthesis mechanism of aluminophosphate molecular sieves. They demonstrated that all the aluminophosphate structures can be derived from the transformation of a parent single chain with corner-sharing Al_2P_2 four-membered rings,[2,5] and, more recently, the one-dimensional growth process has been experimentally validated through in situ SAXS/WAXS techniques (SAXS = small-angle X-ray scattering; WAXS = wide-angle X-ray scattering) by Weckhuysen and co-workers.[6]

Another important aspect of the synthesis mechanism is the role that the organic template plays in the synthesis process. Several mechanisms for templating have been proposed involving hydrogen bonding,[7] the van der Waals shape of the template,[8] and the favored formation of specific structures.[9] Despite these efforts, a thorough understanding of the template effect, particularly the significance of the role of templating in the channel formation of aluminophosphate molecular sieves, is still lacking because of the complexity of the synthesis process.

A very powerful but relatively unexplored way of probing this process is to perform in situ characterization under working conditions.[6,10] In situ characterization of silicalite has been attempted by NMR spectroscopy,[11] SAXS,[12] and X-ray diffraction (XRD).[13] Relatively few in situ studies have been reported in which attempts were made to follow the crystallization of practically used aluminophosphate

[*] F. Fan, Prof. Dr. Z. Feng, Dr. K. Sun, M. Guo, Q. Guo, Dr. Y. Song, Prof. Dr. W. Li, Prof. Dr. C. Li
State Key Laboratory of Catalysis, Dalian Institute of Chemical Physics, Chinese Academy of Sciences, 457 Zhongshan Road, Dalian,116023 (China)
Fax: (+86) 411-8469-4447
E-mail: canli@dicp.ac.cn
Homepage: http://www.canli.dicp.ac.cn
F. Fan, M. Guo, Q. Guo
Graduate University of Chinese Academy of Sciences
Beijing, 100049 (China)

Supporting information for this article is available on the WWW under http://dx.doi.org/10.1002/anie.200903601.

molecular sieves.[4,6,10,11,14,15] Raman spectroscopy is a suitable technique to investigate aqueous solutions as well as solid phases of zeolite synthesis mixtures because of the low Raman scattering cross section of water. We have recently developed an apparatus capable of studying hydrothermal reactions in situ using UV Raman spectroscopy.[16] The results demonstrated that in situ UV Raman spectroscopy could be applied to the study of framework formation in zeolites because of its increased sensitivity and minimal fluorescence interference relative to conventional Raman spectroscopy. It could be anticipated that in situ UV Raman spectroscopy would be a potential tool for the study of the evolution of both the organic templates and inorganic framework simultaneously, which would reveal the interactions between the organic template and framework formation.

We studied, for the first time, the detailed synthesis mechanism of AlPO-5 using in situ UV Raman spectroscopy. A very important intermediate composed of four-membered rings for the channel formation was detected. The intermediate was formed by the templates, which provide steric support for channel formation through their specific molecular vibrations in the very early stages. The building blocks from the intermediate to the final crystals were well characterized by taking advantage of this powerful technique.

The whole hydrothermal synthesis process of AlPO-5 from the precursor to the final crystals was monitored in situ by UV Raman spectroscopy (Figure 1 a). The Raman spectra of the precursors can be divided into three groups: the Raman bands at 370 cm^{-1} correspond to the vibrational modes of isolated octahedral AlO_6 species;[6] the very intense peak at 899 cm^{-1} has been assigned to the symmetric stretching vibration of $P(OH)_3$ in H_3PO_4; all remaining Raman bands at 410, 461, 741, 1016, 1036, 1070, and 1163 cm^{-1} are characteristic of the protonated triethylamine (TEA) template.

A clear view of the intensity changes of the selected Raman bands as a function of time is presented in Figure 1 b. In the time interval between 0 and 100 min, the intensities of Raman bands at 370 and 899 cm^{-1} decrease rapidly and in parallel, indicating the consumption and reaction of the octahedral AlO_6 species and phosphates. Indeed, most of the octahedral AlO_6 species has been consumed and transformed into tetrahedral AlO_4 species before the hydrothermal crystallization event, as demonstrated also by a previous in situ Al K-edge NEXAFS study.[15] This process is well-documented: the phosphoric ions form covalent bonds through bridging oxygen atoms to aluminum atoms by replacing hydroxy groups and breaking Al−O−Al linkages in the raw material.[2,5] Between 100 and 200 min, two Raman bands at 260 and 500 cm^{-1} appear and their intensities

Figure 1. a) UV Raman spectra recorded in situ during crystallization of AlPO-5. The synthesis temperature was 453 K. $\lambda_{ex} = 325$ nm. b) Plots of the intensities of the selected bands as function of time.

increase in parallel. These two bands were assigned to the channel breathing vibrational modes and deformations involving the four-membered rings, respectively.[17] The appearance of the Raman band at 260 cm^{-1} indicates that the synthesis gels are partially crystallized. With prolonged synthesis ($t = 200$–240 min), another new band appeared at 198 cm^{-1}, which can only be found in the well-crystallized sample. In the final stage of the crystallization ($t = 270$–300 min), the intensities of the Raman bands at 198, 260, and 500 cm^{-1} increased further. Furthermore, a shoulder band at 1113 cm^{-1} appeared, and its intensity increased throughout the synthesis process ($t = 0$–270 min). This band was assigned to coupled symmetric stretching modes of individual PO$_4$ and AlO$_4$ tetrahedra in which adjacent tetrahedra vibrate in antiphase.[18] The increasing intensity of the Raman band at 1113 cm^{-1} indicates the increasing numbers of the Al−O−P bonds.

With the evolution of the raw materials and the framework, the most striking changes of the TEA$^+$ templates occurred for the Raman bands at 1016 and 1035 cm^{-1}. The intensities of these bands decreased in the early stages before the appearance of the channel breathing vibrational mode at 260 cm^{-1}, and remained nearly constant as the intensities of the bands at 198, 260, and 500 cm^{-1} increased. Thus, the variations of the two Raman bands at 1016 and 1035 cm^{-1} with the two vibrational modes are closely related to the formation of AFI channels (AFI = AlPO-5).

The Raman bands at 1016 and 1035 cm^{-1} were assigned to the stretching modes of the C−C bond of the three ethyl chains attached to the protonated nitrogen atom of the template.[19] A previous study of the Raman spectra of protonated morpholine constrained in AlPO-34 cages demonstrated that constrained templates are characterized by decreased intensity of the Raman band with the breathing mode accompanied by a small red shift in frequency.[20] In the present study, besides the decreased Raman intensity of these two Raman bands, a small red shift can be observed in the band for TEA containing fully crystallized AlPO-5 after filtration and washing (Figure S1 in the Supporting Information).

The decreasing intensity of the Raman bands at 1016 and 1035 cm^{-1} strongly suggests that template is trapped in the condensed, amorphous aluminophosphate gel. Periodical DFT calculations on the entrapped TEA$^+$ ions also indicated that the molecular diameter of the TEA$^+$ ions is reduced by 4% and 10% in volume when constrained in the channel; these results are in good agreement with the Raman results (Figure 2).
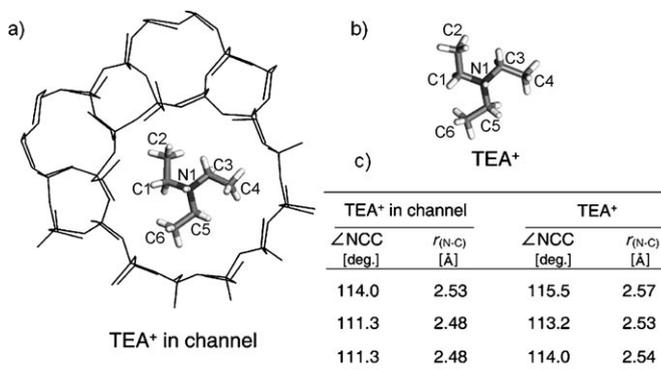
Figure 2. Periodic DFT-optimized structure of a) the encapsulated protonated triethylamine in the AFI channel and b) protonated triethylamine. c) Comparison of ∡CNN and $r_{(C-N)}$ (the distance between the N atom and the methyl carbon atom) between (a) and (b).

TEA$^+$ in channel		TEA$^+$	
∠NCC [deg.]	$r_{(N-C)}$ [Å]	∠NCC [deg.]	$r_{(N-C)}$ [Å]
114.0	2.53	115.5	2.57
111.3	2.48	113.2	2.53
111.3	2.48	114.0	2.54

It is worth noting that the intensities of these two Raman bands remained almost constant during the formation of the crystalline AFI channels. The results show that the templates are less affected by the surrounding environment during the formation of the crystalline channel. A plausible explanation is that a channel-like structure had already been formed before the formation of the crystalline channels. Corma and co-workers predicted that an assembled organic–inorganic

amorphous material containing the appropriate pore dimensions and topologies may be formed in the early stages of zeolite synthesis and that this amorphous materials will subsequently be transformed into ordered (crystalline) nucleus and then zeolite crystals.[21,22]

To validate the existence of the channel-like structure in the early stages of synthesis, Fe^{3+}/H_2O_2 (Fenton's reagent) was used to remove the TEA template at room temperature[23] and prevent the breakdown of the pores and coke formation during calcination. Figure 3a shows the pore size distributions of AlPO-5 and the intermediates crystallized for 100 min (before the formation of the crystalline channel), as determined by Raman spectroscopy. Amorphous intermediates gave pore size distribution maximum at 8.9 Å, whereas the fully crystallized AlPO-5 gave pore size distribution maximum at 7.3 Å. The above results show that the amor-

phous intermediates already have some microporous properties before the formation of the crystalline channels. The micropore volume ratio of the intermediate to the final product is approximately 7% (Table 1 in the Supporting Information). The low porosity ratio indicated that these channel-like intermediates are not well-developed 3D architectures.

To further clarify the nature of the evolution of the inorganic phase, the templates of AlPO-5 synthesized at various stages were removed with Fenton's reagent and the products were characterized by UV Raman spectroscopy (Figure 3b). The Raman spectrum of the sample crystallized for 50 min showed the appearance of the two broad Raman bands at 296 and 504 cm^{-1}. After 100 min, the intensities of these two Raman bands increased and varied in parallel. Between 150 and 300 min, the broad Raman band at 504 cm^{-1} grew and gradually shifted to 500 cm^{-1}. The appearance of the broad Raman band at 504 cm^{-1} suggests the formation of distorted four-membered rings in the very early stages of the synthesis, which can be understood by considering Oliver's 1D chain model with corner-sharing Al_2P_2 four-membered rings.[5] Two Raman bands appeared at 260 and 399 cm^{-1} and grew considerably with increasing synthesis time. Notably, the growing Raman band at 260 cm^{-1} was accompanied by a decrease in the intensity of the broad Raman band at 296 cm^{-1}. This result indicates that the crystalline channel structure is derived from the species characterized by the broad Raman band at 296 cm^{-1}. Thus, the broad Raman band at 296 cm^{-1} is attributed to the existence of the channel-like structures in amorphous phase.

The Raman band at 399 cm^{-1} appeared and varied in parallel with the Raman band at 260 cm^{-1} due to the breathing modes of the crystalline channel. It is known that the frequency of the ν_s(T-O-T) mode has an inverse dependence on the magnitude of the average T-O-T angle.[24] The ideal candidate for the vibration modes of the Raman band at 399 cm^{-1} is the six-membered ring. Periodical DFT calculations confirmed that the frequency of the breathing vibration mode of the six-membered rings is around 387 cm^{-1}.

It should be noted that the four-membered-ring species formed in the very early stages of the synthesis participate in the formation of channel-like structures, whereas the appearance of the newly formed six-membered rings is crucial for the formation of the crystalline channel. The latter process is also supported by the theoretical model proposed by Oliver et al.,[5] which demonstrated that removal of the caps in the capped six-membered rings and interlayer condensation resulted in the formation of new six-membered rings and a crystalline AFI structure.

By combining the information obtained from the previously studies,[5,6,15] we propose the following synthesis mechanism for AlPO-5 (Figure 4). In the very early stages, the aluminates and phosphates react to form amorphous aluminophosphate gel phase with some of the octahedral AlO_6 species, thereby transforming into tetrahedral AlO_4 species. Subsequently, the formation of the Al—O—P bonds follows a one-dimensional growth process, as proved by previous work.[6] The UV Raman results show that these one-dimensional chains contain four-membered rings. The cationic
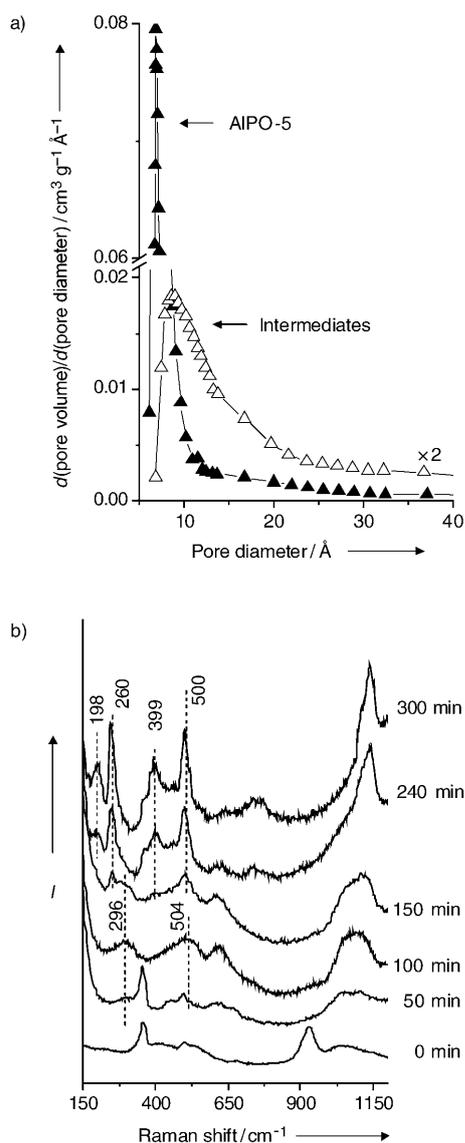
Figure 3. a) Pore size distribution based on N_2 physisorption: △ sample crystallized for 100 min, ▲ fully crystallized AlPO-5; b) UV Raman spectra with excitation at 266 nm of AlPO-5 showing different crystallization stages at various times of the synthesis.

Communications
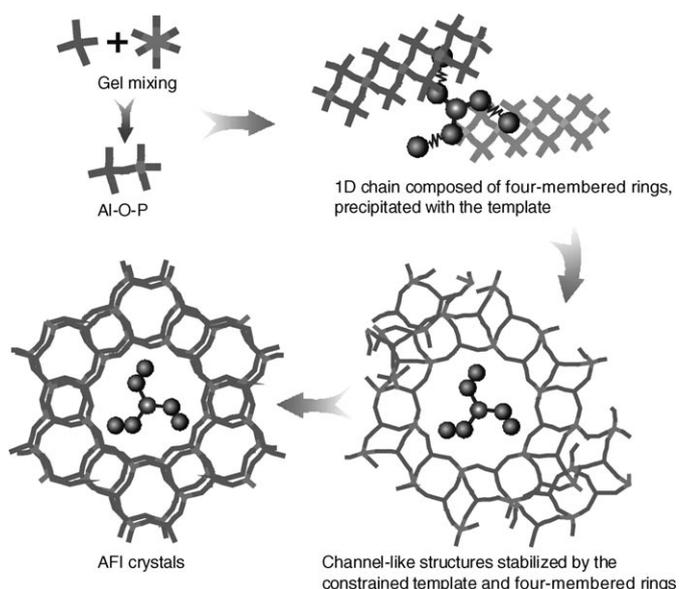
Figure 4. A proposed synthesis mechanism of AlPO-5.

templates reduce the interchain electrostatic repulsion, allowing them to crystallize from solution. With increasing synthesis time, during the condensation of these chains composed of four-membered rings, channel-like structures are formed in the amorphous phase and stabilized by the steric effect of the template. With prolonged synthesis time, these poorly crystallized channel-like structures reconstruct through intra- and interchain rearrangements of the 1D chains to form crystalline channels by the newly formed six-membered rings.

In summary, in situ UV Raman spectroscopy in combination with the Fenton reaction provides direct evidence for the existence of the four-membered ring species in the very early stages of the synthesis. The condensation of the four-membered ring species with the steric role of the organic templates resulted in an amorphous pre-state with channel-like structures, which subsequently transform into 3D AFI architectures via the newly formed six-membered rings. This work provides molecular-level insights into the role of the template played in channel formation as well as the identification of the building blocks during the framework formation. We anticipate that this work will facilitate the choice of organic templates and tailoring the building blocks for the rational synthesis of zeolites.

Experimental Section

Characterization: Nitrogen adsorption and desorption isotherms at 77 K were measured using a Micromeritics ASAP 2020M system. The samples were degassed for 10 h at 150°C before the measurements. The porosity was analyzed by N_2 physisorption. The pore size distribution was calculated according to the Horvath–Kawazoe model applied to the adsorption branch of the isotherm.

UV Raman spectra were recorded on a home-assembled UV Raman spectrograph using a Jobin–Yvon T64000 triple-stage spectrograph with spectral resolution of 2 cm^{-1}. The laser line at 325 nm of a He–Cd laser was used as an excitation source at an output of 50 mW.

The power of the laser at samples was about 1.0 mW. The 266 nm line from the double frequency of Coherent Verdi-V10 laser through WaveTrain CW frequency doubler was used as another excitation source. The power of the 266 nm line at samples was below 1.0 mW.

[1] a) R. H. Jones, J. M. Thomas, R. R. Xu, Q. S. Huo, Y. Xu, A. K. Cheetham, D. Bieber, *J. Chem. Soc. Chem. Commun.* **1990**, 1170–1172; b) T. Loiseau, F. Serpaggi, G. Ferey, *Chem. Commun.* **1997**, 1093–1094; c) A. A. Ayi, S. Neeraj, A. Choudhury, S. Natarajan, C. N. R. Rao, *J. Phys. Chem. Solids* **2001**, *62*, 1481–1491; d) L. Yu, W. Pang, L. Li, *J. Solid State Chem.* **1990**, *87*, 241–244.

[2] S. Oliver, A. Kuperman, A. Lough, G. A. Ozin, *Chem. Mater.* **1996**, *8*, 2391–2398.

[3] a) P. A. Barrett, R. H. Jones, *J. Chem. Soc. Chem. Commun.* **1995**, 1979–1981; b) J. M. Thomas, R. H. Jones, R. R. Xu, J. S. Chen, A. M. Chippindale, S. Natarajan, A. K. Cheetham, *J. Chem. Soc. Chem. Commun.* **1992**, 929–931; c) K. X. Wang, J. H. Yu, Y. Song, R. R. Xu, *Dalton Trans.* **2003**, 99–103; d) J. Yu, R. Xu, *Acc. Chem. Res.* **2003**, *36*, 481–490.

[4] T. Loiseau, L. Beitone, F. Millange, F. Taulelle, D. O'Hare, G. Ferey, *J. Phys. Chem. B* **2004**, *108*, 20020–20029.

[5] S. Oliver, A. Kuperman, G. A. Ozin, *Angew. Chem.* **1998**, *110*, 48–64; *Angew. Chem. Int. Ed.* **1998**, *37*, 46–62.

[6] D. Grandjean, A. M. Beale, A. V. Petukhov, B. M. Weckhuysen, *J. Am. Chem. Soc.* **2005**, *127*, 14454–14465.

[7] M. E. Davis, R. F. Lobo, *Chem. Mater.* **1992**, *4*, 756–768.

[8] D. W. Lewis, C. M. Freeman, C. R. A. Catlow, *J. Phys. Chem.* **1995**, *99*, 11194–11202.

[9] S. A. Pelster, W. Schrader, F. Schuth, *J. Am. Chem. Soc.* **2006**, *128*, 4310–4317.

[10] M. G. O'Brien, A. M. Beale, C. R. A. Catlow, B. M. Weckhuysen, *J. Am. Chem. Soc.* **2006**, *128*, 11744–11745.

[11] O. B. Vistad, D. E. Akporiaye, F. Taulelle, K. P. Lillerud, *Chem. Mater.* **2003**, *15*, 1639–1649.

[12] a) P. de Moor, T. P. M. Beelen, R. A. van Santen, K. Tsuji, M. E. Davis, *Chem. Mater.* **1999**, *11*, 36–43; b) W. Fan, M. Ogura, G. Sankar, T. Okubo, *Chem. Mater.* **2007**, *19*, 1906–1917.

[13] F. Rey, G. Sankar, J. M. Thomas, P. A. Barrett, D. W. Lewis, C. R. A. Catlow, S. M. Clark, G. N. Greaves, *Chem. Mater.* **1995**, *7*, 1435–1436.

[14] a) B. M. Weckhuysen, D. Baetens, R. A. Schoonheydt, *Angew. Chem.* **2000**, *112*, 3561–3564; *Angew. Chem. Int. Ed.* **2000**, *39*, 3419–3422; b) P. Norby, A. N. Christensen, J. C. Hanson, *Inorg. Chem.* **1999**, *38*, 1216–1221; c) G. Muncaster, A. T. Davies, G. Sankar, C. R. A. Catlow, J. M. Thomas, S. L. Colston, P. Barnes, R. I. Walton, D. O'Hare, *Phys. Chem. Chem. Phys.* **2000**, *2*, 3523–3527.

[15] A. M. Beale, A. M. J. van der Eerden, D. Grandjean, A. V. Petukhov, A. D. Smith, B. M. Weckhuysen, *Chem. Commun.* **2006**, 4410–4412.

[16] F. T. Fan, Z. C. Feng, G. N. Li, K. J. Sun, P. L. Ying, C. Li, *Chem. Eur. J.* **2008**, *14*, 5125–5129.

[17] A. J. Holmes, S. J. Kirkby, G. A. Ozin, D. Young, *J. Phys. Chem.* **1994**, *98*, 4677–4682.

[18] J. A. Creighton, H. W. Deckman, J. M. Newsam, *J. Phys. Chem.* **1991**, *95*, 2099–2101.

[19] C. Gobin, P. Marteau, J.-P. Petitet, *Spectrochim. Acta Part A* **2004**, *60*, 329–336.

[20] L. Marchese, A. Frache, E. Gianotti, G. Martra, M. Causa, S. Coluccia, *Microporous Mesoporous Mater.* **1999**, *30*, 145–153.

[21] A. Corma, M. J. Diaz-Cabanas, *Microporous Mesoporous Mater.* **2006**, *89*, 39–46.

[22] a) A. Corma, M. Moliner, M. J. Diaz-Cabanas, P. Serna, B. Femenia, J. Primo, H. Garcia, *New J. Chem.* **2008**, *32*, 1338– 1345; b) A. Corma, M. J. Diaz-Cabanas, M. Moliner, G. Rodriguez, *Chem. Commun.* **2006**, 3137–3139.

[23] I. Melian-Cabrera, F. Kapteijn, J. A. Moulijn, *Chem. Commun.* **2005**, 2744–2746.

[24] P. K. Dutta, D. C. Shieh, M. Puri, *Zeolites* **1988**, *8*, 306–309.